Modeling X-ray Emissions from Rocket Triggered Lightning

A Thesis Submitted in Partial Satisfaction Of the Requirements for the Degree of Bachelor of Science in Physics at the University of California, Santa Cruz

Andrew Reid

6 June, 2011

Adriane Steinacker
Senior Theses Coordinator

David Smith
Technical Advisor

David P. Belanger
Chair, Department of Physics

Table of Contents

Abstract

Recent observations have been made of X-ray emissions from natural lightning. Shortly after, observations of X-ray emissions from rocket triggered lightning, an analogous process (described in Part I), were made. Typical NaI(Tl) detector instruments have relatively slow response times and when detecting large bursts of energetic radiation, cannot resolve individual photons to determine an emission spectrum. Using Monte Carlo simulations, we can model X-rays passing through the X-CAM detector used at the University of Florida's lightning research facility (Camp Blanding). We can then compare theoretical input models with real camera images and make some assumptions about the emission spectrum. This may reveal information about the stepping nature of the leader phases of lightning, something not well understood. The results of some preliminary tests are presented in Part II.

Part I
Introduction

Lightning is a complex atmospheric phenomenon. Part of the challenge in studying lightning is the guesswork involved in predicting the precise location and time of a strike. For this reason, the technique of rocket-triggered lightning has provided researchers with excellent opportunity to study lightning. Rocket-triggered lightning works as follows: a rocket is launched from a tower into a thunderstorm above trailing a conductive copper wire connecting to the ground. In a successful launch, the rapid introduction of the wire into the cloud creates a negative discharge from cloud to ground. The photograph in figure 1 was taken at a University of Florida research facility in Camp Blanding, Florida.

Figure 1: A rocket-triggered strike at Camp Blanding, Florida [*source*: lightning.ece.ufl.edu].

This is analogous to natural negative cloud to ground lightning. The process of natural lightning begins with charge separation occurring within a cloud, leaving a positively charged top layer and a negatively charged bottom layer.

An initial breakdown occurs which "can be viewed as a discharge process between the negative and lower positive charge regions, but it can also involve a sequence of channels extending in random directions from the cloud charge source" [Baba, 2009]. The plasma channel that bridges the cloud to ground is known as the stepped leader, moving at an average velocity of $2x10^5$ m/s in a series of ~1 μs steps [Baba, 2009]. The stepped leader initiates the upward moving return stroke. Following this is a downward moving dart leader, following the ionized pathway created by the return stroke. The dart leader/return stroke sequence can repeat multiple times. The net effect of this is negative charge being transferred from the cloud to the ground.

Rocket triggered lightning follows a slightly different progression, but with many similar features. No stepped leaders are typically present, the process begins with a dart leader, following the trailing rocket wire. A return stroke then follows the dart leader. The process may repeat following the dart leader/return stroke sequence.

1.1 X-ray emissions from lightning

Natural lightning was first observed to produce energetic radiation by Moore et al. (2001). Researchers at the University of Florida have found that triggered lightning can also produce bursts of X-ray radiation [Dwyer et al., 2003]. A typical lightning stroke has a temperature around 30,000 K [Saleh et al., 2009], not nearly hot enough for thermal effects to produce X-ray radiation. During the stepped leader propagation, the electric field (integrated $\frac{dE}{dt}$) waveform drops as negative charges suddenly jump towards the ground in discrete steps (on the order of 10 μs) [Dwyer, 2009]. It is believed that the tips of the leaders produce X-rays and that the stepping process involves the production of runaway electrons, which are accelerated by large electric fields to relativistic energies [Dwyer 2009; Gurevich and Zybin, 2001; Dwyer, 2003, 2004]. As these runaway electrons collide with air molecules, they may knock off secondary runaway electrons, creating an avalanche effect. They slow down (from air collisions) and emit bremsstrahlung radiation in a short region near the leader tip [Saleh et al., 2009]. Dwyer et al. (2003) observed X-ray emissions from *rocket triggered* lightning during the dart leader phase, this implies that the dart leader process involves stepping to some degree as well. A simplified schematic of this is shown in figure 2 below.

Figure 2: A simplified schematic of a dart leader emitting X-rays [Saleh et al., 2009].

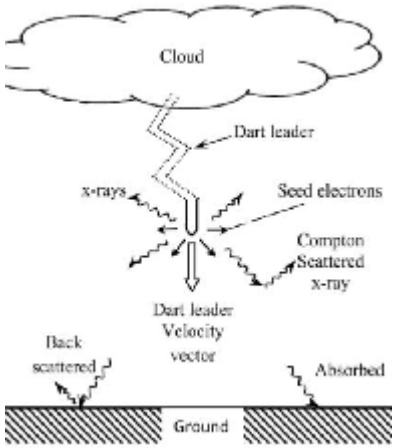

1.2 Gamma-ray emissions

In addition to X-ray emissions, a gamma-ray flash was observed by Dwyer et al. (2004). They reported an intense gamma-ray burst (with some photon energies exceeding 10 MeV), lasting for around 300 μs [Dwyer et al., 2004]. The flash was observed 650 m from the lightning channel by three different X-ray cameras. The lightning was rocket-triggered, and occurred at a time consistent with the initial stages of triggered lightning. When the rocket reaches a sufficient height, an upward moving positive leader is initiated between the tip of the rocket and the cloud overhead (6-8 km). The large discharge might then produce runaway electrons, and produce gamma-rays [Dwyer, 2009]. This mechanism is distinctly different from the process described in section 1.1, this radiation is associated with an upward moving leader rather than a downward moving one.

Terrestrial gamma-ray flashes (TGF's) have been observed in space by the Compton Gamma Ray Observatory satellite [Fishman et al., 1994]. Smith et al. (2005) observed TGF's collected by the RHESSI spacecraft. Dwyer and Smith (2005) used Monte Carlo simulations modeling runaway electrons to fit the origin of emission in the 15-21 km range. This makes it a possibility that the source of these emissions is from thunderclouds, as the tops of thunderclouds are typically 15 km from the ground [Williams et al., 2006].

1.3 Detection instruments

NaI crystals (used as scintillators) coupled to photomultiplier tubes (PMTs) are common detection instruments. When an X-ray enters a crystal (or any material for that matter), three things can happen. The photon can Compton scatter and deposit some of its energy into a recoil electron via equation 1:

$$\frac{1}{E_f} - \frac{1}{E_i} = \frac{1}{m_e c^2}(1 - \cos\theta) \text{ [1]}$$

Where E_i is the incident photon energy, E_f is the scattered photon energy, m_e is the electron mass, c is the speed of light, h is the Planck constant and θ is the recoil angle of the photon. Alternatively, the photon could undergo the photoelectric effect, where the crystal completely absorbs the photon and emits an electron with an energy determined by the absorbed photons energy. The following equation relates the maximum kinetic energy of the electron (K_0), to the frequency of the absorbed photon (ν) and the work function of the material (W):

$$K_0 = h\nu - W \text{ [2]}$$

A third process, namely pair production, could occur as well. This happens when a photon-nucleus collision produces an electron and its antiparticle, a positron. They soon annihilate one another and emit two 511 keV photons (equal to the rest mass of an electron). These secondary photons could then go on to Compton scatter or undergo photoelectric absorption. All of these processes can excite free electrons in the valence band of an NaI crystal to higher energy levels. The NaI crystals are doped with an impurity, such as thallium, adding transitional levels between the valence and conduction band. Electron hole pairs move through the crystal and eventually decay, emitting scintillation photons in the process. A PMT is mounted beneath a crystal to absorb the scintillation photons. A PMT consists of a series of charged plates, each plate at a higher voltage than the last. The scintillation photon strikes the cathode, where electrons are emitted via the photoelectric effect. These electrons are drawn into the next plate (first dynode) where secondary electrons are emitted and drawn to the next dynode. Typically a PMT contains multiple (~10) dynodes. Finally, the last plate (anode) collects all of the electrons, generating a current proportional to the flux of initial incoming scintillation photons. One ends up with a signal, plotting voltage vs. time. Figure 3 shows a detector response.

Figure 3: A NaI/PMT response to a leader step [Dwyer et al. 2003]. The control PMT (blue line) had no mounted NaI scintillator.

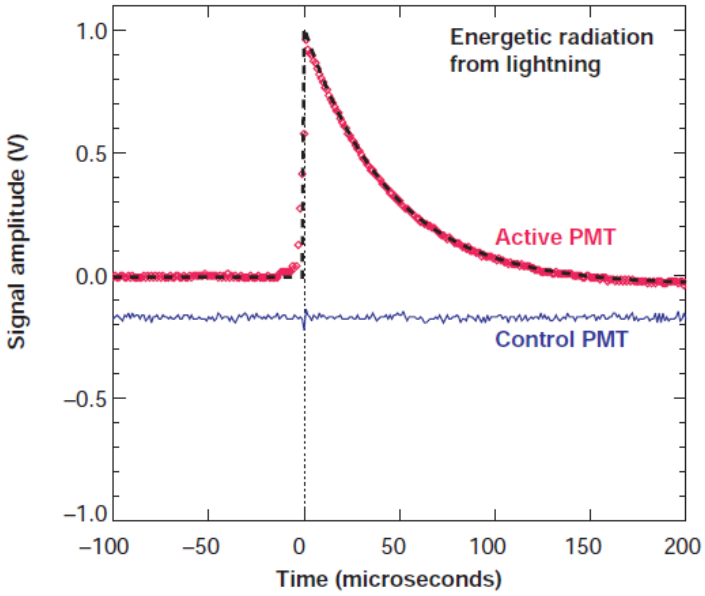

While one can determine the total energy deposited in a detector, there is no indication of what the spectrum looks like. Each step deposits large amounts of energy ($>$ 10 MeV) into the crystals and a typical burst will last somewhere on the order of 100 μs [Dwyer et al., 2003]. This is comparable to a NaI scintillators relaxation time and thus one cannot resolve individual photons to determine an emission spectrum. The goal of this research is ultimately to determine a realistic spectrum using computer modeling and simulations, described in more detail in Part II.

Part II
Monte Carlo simulations

Monte Carlo modeling methods can be used to simulate the passage of X-rays through a detector. All of the relevant physics described in the previous section is handled in the GEANT3 [13] software package used for simulation. The simulation, for example, includes Compton scattering, Rayleigh scattering, pair production, and the photoelectric effect. One can make quite detailed geometries and model a detector with good accuracy. The simulation modeled the X-CAM detector used by Dwyer et al. in Camp Blanding, Florida [12]. The X-CAM (short for X-ray camera) consists of thirty NaI/PMT detectors housed in a lead

box (to screen out background radiation and light), with a square pinhole at the front of the camera. Figure 4 shows the X-CAM and a graphical representation of the model.

Figure 4: Figures 4a/c show the model and figures 4b/d show the X-CAM. One can see the array of NaI detectors in figures 4a and 4b [12].

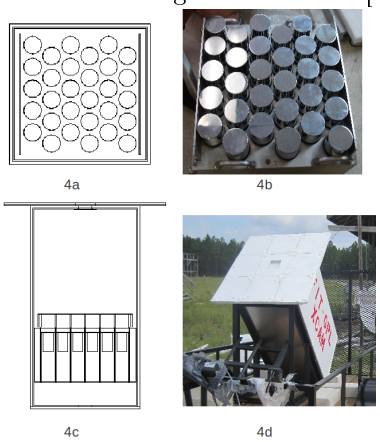

Figure 5 shows the X-CAM's response to a real lightning strike. Note that this is a still frame taken from an animation created by Joseph Dwyer [Florida Institute of Technology].

Figure 5: Individual detector responses to a real strike [J. Dwyer, 2010 AGU Fall meeting]

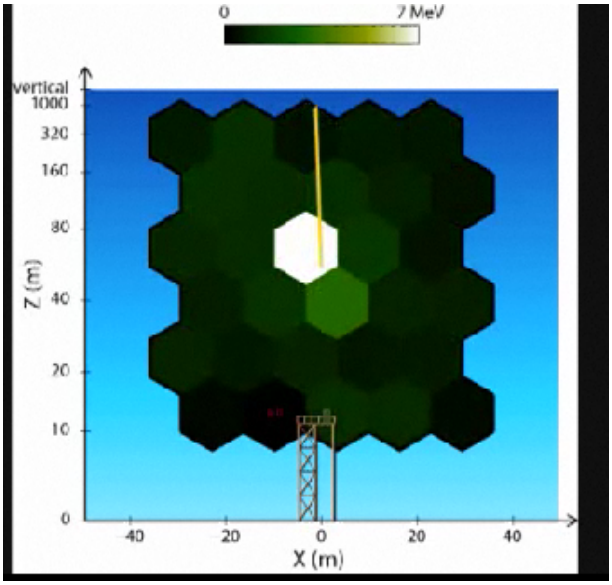

One can see the very brightly illuminated central detector, but as time progresses, this changes. If X-rays are emitted from the leader head as predicted, the emission point will drop towards the tower as time progresses. Evidence of this is seen in the animation, the most brightly illuminated detectors are in the top region of the camera, and as time progresses, the lower detectors become illuminated. We will attempt to explain aspects of X-CAM responses with GEANT3 simulations. The spectrum and emission height will be varied and compared to real responses.

2.1 Preliminary Tests

This model was first placed in a small air filled environment. A stream of 1 MeV photons was triggered from just above the camera face. The photons were triggered randomly from a hemisphere above the camera. GEANT tracks each photon and records the camera region where it is absorbed. The NaI crystals are the region of interest, this is where scintillation photons are produced which are collected by the PMT. The output file contained the spectrum (energy and photon count) for each of the thirty NaI crystals. As a test, the lead thickness of the top plate was varied, and the results were plotted together in figure 6.

Figure 6: Total energy (keV) deposited in each detector for three different plate thicknesses.

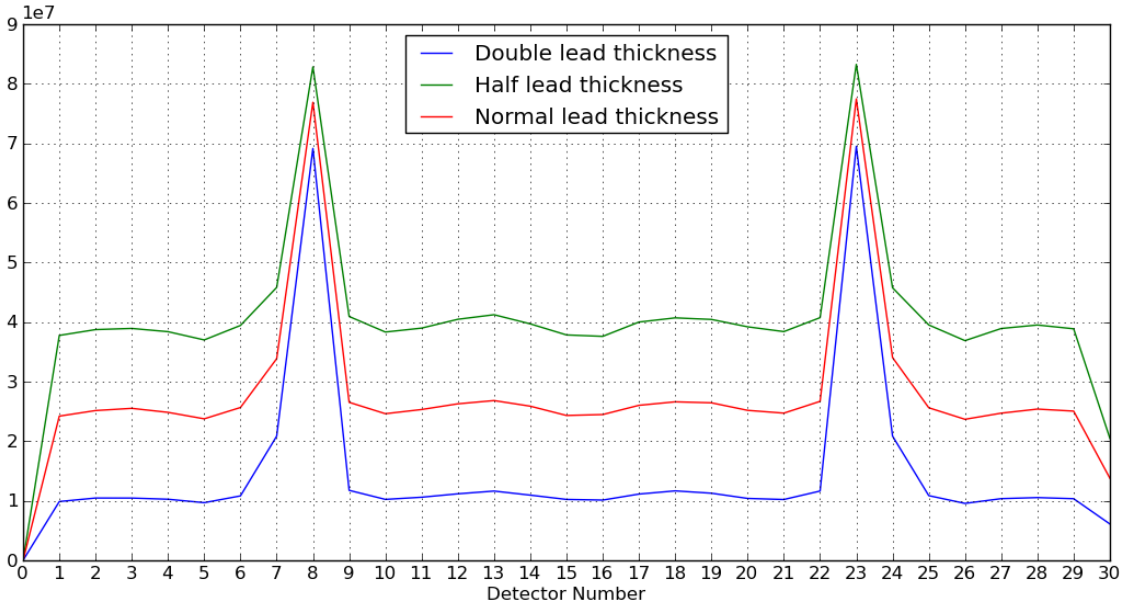

The two detectors that clearly stand out are the two central detectors (8 and 23), which sit directly beneath the square camera pinhole. The top lead plate shields the detectors, and as its thickness is increased, the total energy deposited in every detector dropped. When examining the non-central detectors, certain detectors receive more energy than others. There seems to be a symmetry about the first half (detectors 1-15) and the last half (16-30). Figure 7 shows, for reference, the geometrical array of the thirty detectors. A color intensity has been added to show which detectors received the most energy. The darker the shade of green, the more energy deposited. The two central detectors stand out greatly (by roughly a factor of 2) from the rest, so their intensities were left out of the calculation and were instead denoted with a * and a lightly tinted color.

Figure 7: A color map of the detector array, with a normal thickness top plate.

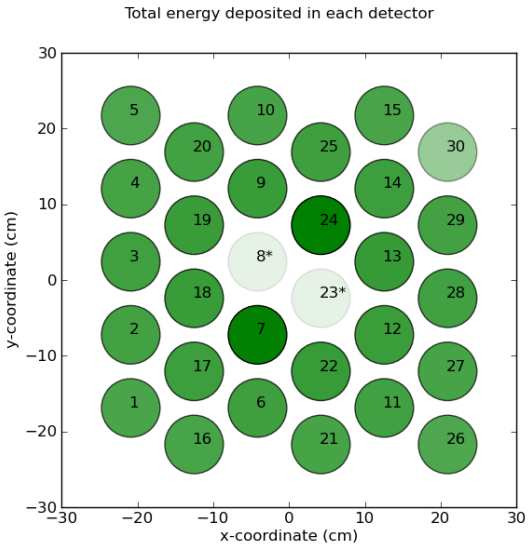

This is a similar map to Dwyer's (figure 5), but differs in a number of ways. This, right now, is a very simplified model. Each photon was triggered with an energy of 1 MeV and there was no long range air interaction. The photons were angled at the XCAM head on, and triggered from a small distance above the cameras top plate. The model was placed in an environment soley consisting of air. Figure 8 shows the total counts each detector received in the 1 MeV photopeak.

Figure 8: Total counts in the photopeak for each detector, with varying top plate thicknesses.

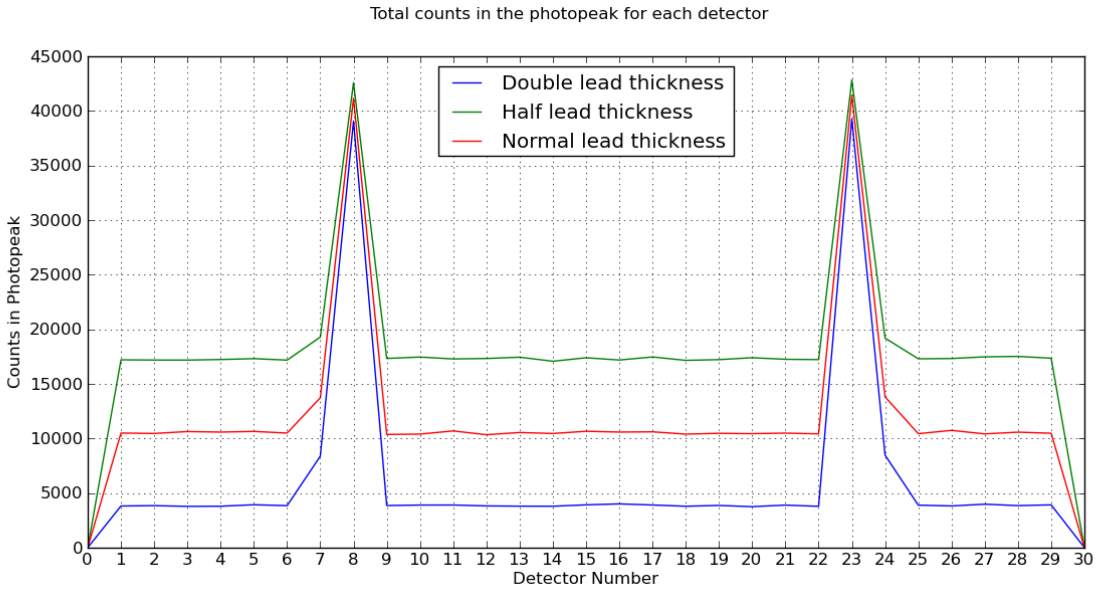

The differences between this plot and the previous (figure 6) are clear. When one excludes photons that scattered (lowering their energy out of the photopeak), the non-central detectors appear to receive roughly the same number of counts. The two detectors adjacent to the central detectors (7 and 24) are slightly less shielded than their neighbors, but still much more shielded relative to the two central detectors (8 and 23). Detector 30 received zero counts in the photopeak. Figure 9 illustrates this.

Figure 9: A color map of the detector array, with a normal thickness top plate.

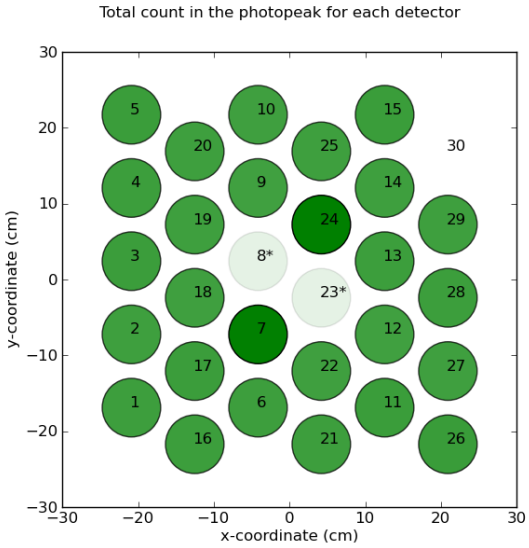

As another test, photons were targeted directly at one of the central detectors (detector 8), again, all triggered with a uniform energy of 1 MeV and varying lead thicknesses. Figure 10 shows a plot of the total energy deposited for each detector.

Figure 10: Total energy (keV) deposited in each detector, with varying lead thicknesses and with the photons targeted at detector 8.

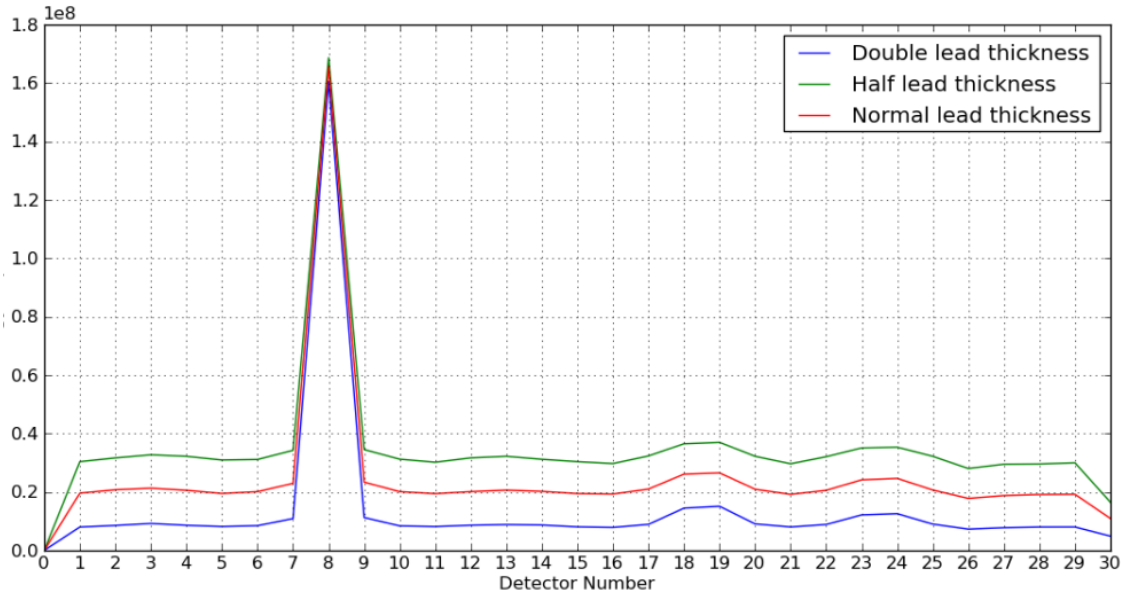

As expected, detector 8 received the most energy in all cases. Detectors 7, 9, 18, 19, 23, and 24 stand out as being unique as well. For some reason, these detectors received more scattered photons than their shielded neighbors. It could have been the case that photons were being scattered by detector 8 into 18 and 19. Detectors 23 and 24 sit to the right of detector 8, and appeared to receive some backscattered photons. Detectors 7 and 9, as one might expect, sit above and below detector 8, and receive some scattered photons as well. One can see this in figure 11.

Figure 11: Color map of the detector array, with a normal thickness top plate. Photons were targeted at detector 8.

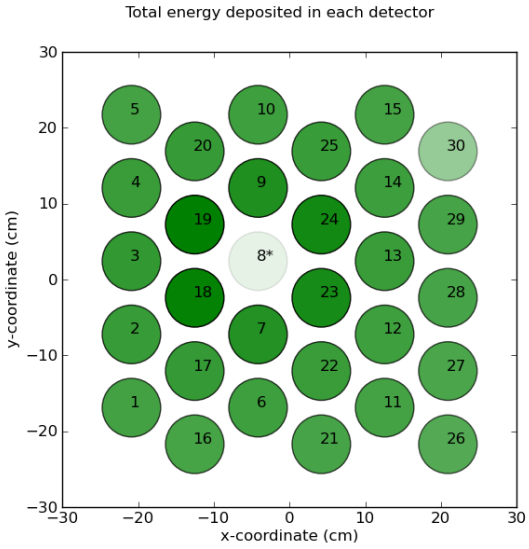

As was done previously, a plot was created showing the total photopeak count for each detector. Figure 12 shows the results.

Figure 12: Total counts in the photopeak for each detector, with varying lead thicknesses. The photons are targeted at detector 8.

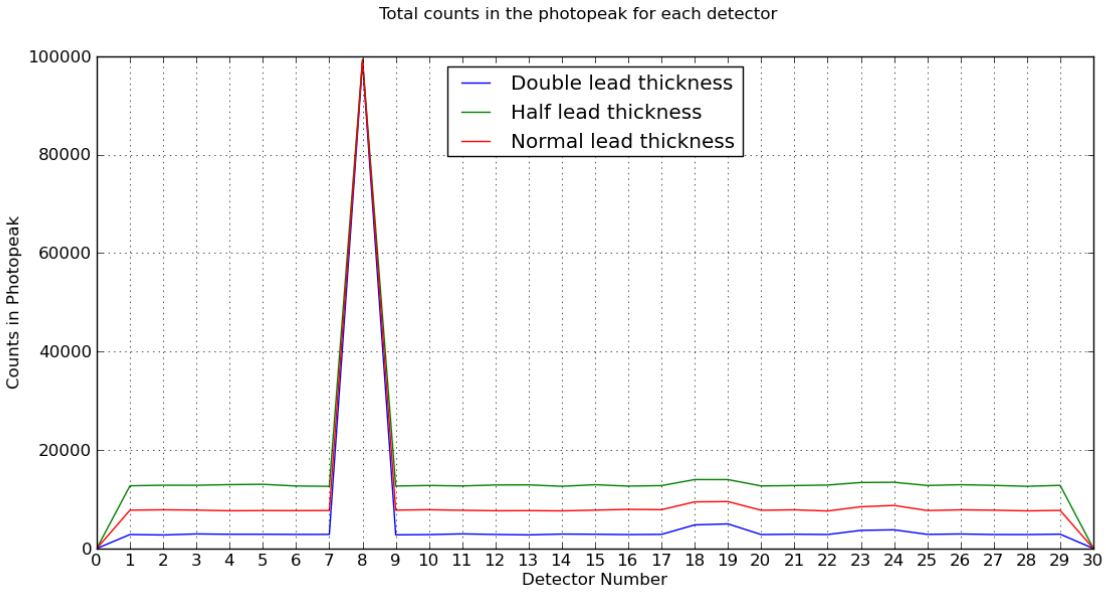

Unlike the previous photopeak plot, two non-central detectors still slightly stand out from the rest. Detectors 18 and 19 received more counts, and this makes sense. These two detectors sit directly to the left of detector 8 (the target detector) and the angled spectrum, while shining mostly on detector 8, also shines a slightly higher number of photons at these two detectors. Figure 13 illustrates this.

Figure 13: Color map of the detector array, with a normal thickness top plate. Photons were targeted at detector 8.

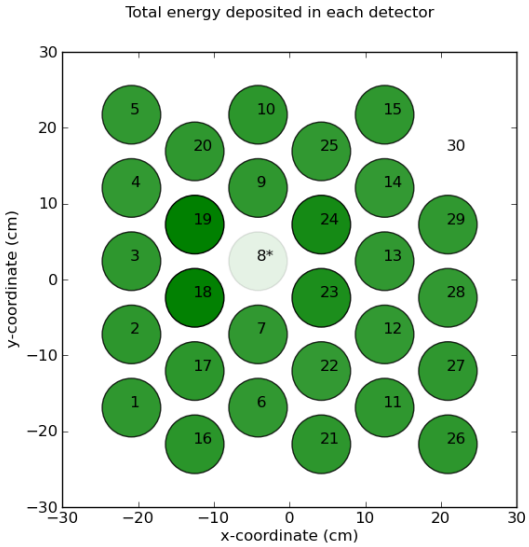

In summary, the effect of varying the lead thickness is just what one would predict. With a thicker lead plate, fewer photons make it to the detector crystals and more scattering occurs. Detector 30, in all situations, received the fewest photons (both scattered and in the photopeak). This should not occur since there is a geometrical symmetry between detectors 1 and 30 (see figure 7). There is a strong probability that an asymmetry was unintentionally introduced into the model. This is something that still needs to be corrected.

2.2 Long range air interaction and other future simulations

The next step is to include a long range air interaction in the simulation. Atmospheric scattering is important, and should not be ignored when modeling X-ray passage through a camera. The X-CAM sits roughly 50 meters from the lightning channel where the intensity of X-rays is observed to be the greatest [Dwyer et al., 2004]. At this distance, atmospheric scattering plays a large role in what the camera sees. This is analogous to the results found in section 2.1, only instead of varying the lead thickness, we will increase the air distance between the camera and emission point. The effect of this should be less counts in the photopeak and more lower energy scattered photons deposited into each detector. The difficulty with this is that the computer must spend time tracking wandering photons in air, which has a relatively low density. Photons often travel large distances before becoming completely absorbed and are tracked by the computer until they fall below some cutoff energy. While one can raise the cutoff energy, this makes the simulation less realistic, as some of these cutoff photons could potentially find their way into a detector. We are still working on solving this problem, so we can trigger enough photons to get good counting statistics.

Once we collect simulation data with a long range air interaction, we will vary the emission spectrum. A continuous 1 MeV distribution of X-rays is probably not realistic, it is more likely the case that some higher and lower energy photons are emitted as well. It is thought that X-rays are emitted isotropically from the leader [Saleh et al., 2009], and we will use this assumption in our model. The camera images (from the real camera) are going to be compared with theoretical input models, and tested with a chi-square method. This will allow us to make inferences about the X-ray spectrum associated with lightning leaders and the stepping process.

References

[1] Dwyer et al 2003: "Energetic Radiation Produced by Rocket-Triggered Lightning", Science, 299, 694-697, 2003, J.R. Dwyer, M.A. Uman, H.K. Rassoul, M. Al-Dayeh, E.L. Caraway, J. Jerauld, V.A. Rakov, D.M. Jordan, K.J. Rambo, V. Corbin, and B. Wright.

[2] Saleh et al: "Properties of the x-ray emission from rocket-triggered lightning as measured by the Thunderstorm Energetic Radiation Array

(TERA)", J. Geophys. Res. Vol. 114, D17210, doi:10.1029/2008JDO11618, 2009, Z. Saleh, J. Dwyer, J. Howard, M. Uman, M. Bakhtiari, D. Concha, M. Stapleton, D. Hill, C. Biagi and H. Rassoul

[3] Yoshihiro Baba and Vladimir A. Rakov, Present Understanding of the Lightning Return Stroke (from H.D. Betz et al. (eds), Lightning: Principles, Instruments and Applications, doi: 10.1007/978-1-4020-9079-0_1, Springer Science+Business Media B.V. 2009.)

[4] Joseph R. Dwyer, Energetic Radiation and Lightning (from H.D. Betz et al. (eds), Lightning: Principles, Instruments and Applications, doi: 10.1007/978-1-4020-9079-0_1, Springer Science+Business Media B.V. 2009.)

[5] Fishman, G.J. et al., Discovery of intense gamma-ray flashes of atmospheric origin, Science, 264, 1313, 1994.

[6] Smith, D.M., L. I. Lopez, R. P. Lin. C. P. Barrington-Leigh, Terrestrial Gamma-Ray Flashes observed up to 20 MeV, Science, 307, 1085-1088, 2005.

[7] Dwyer, J. R., and D. M. Smith, A Comparison between Monte Carlo simulations of runaway breakdown and terrestrial gamma-ray flash observations, Geophys. Res. Lett., 32 L22804, doi:10.1029/2005GL023848, 2005.

[8] Williams E., et al., Lightning Flashes Conductive to the Production and Escape of Gamma Radiation to Space, J. Geophys. Res., 111, Issue D16, CiteID D16209, 2006.

[9] Moore, C.B.,K.B. Eack, G.D. Aulich, and W. Rison, Energetic radiation associated with lightning stepped-leaders, Geophys. Res. Lett., 28, 2141-2144, 2001.

[10] Gurevich, A. V., and K. P. Zybin (2001), Runaway breakdown and electric discharges in thunderstorms, Phys. Uspekhi, 44, 1119 – 1140.

[11] Dwyer, J. R. (2004), Implications of x-ray emission from lightning, Geophys. Res. Lett., 31, L12102, doi:10.1029/2004GL019795

[12] Images in figure 4 and XCAM drawings provided by Joseph Dwyer, Florida Institute of Technology, 2010.

[13] GEANT3 documentation: http://wwwkph.kph.uni-mainz.de/computing//docu/geant/Geant-HTML/geantall.htm. CERN, 1993.